

Fig. S1: ATR-FTIR spectrum of DGAMA-OCT & DGAMA-APTES-OCT

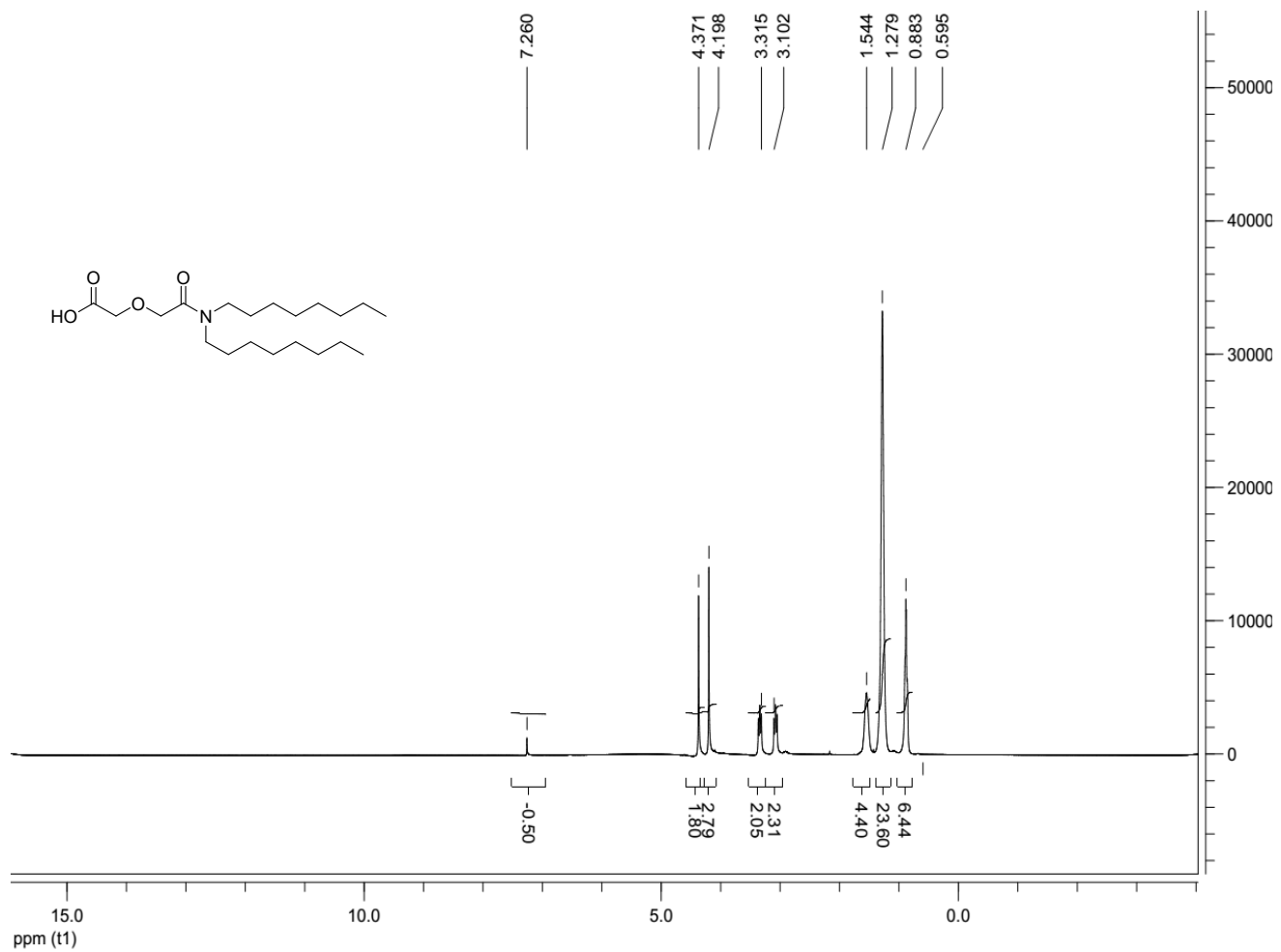


Fig. S2: <sup>1</sup>H-NMR spectra for DGAMA-OCT in CDCl<sub>3</sub>

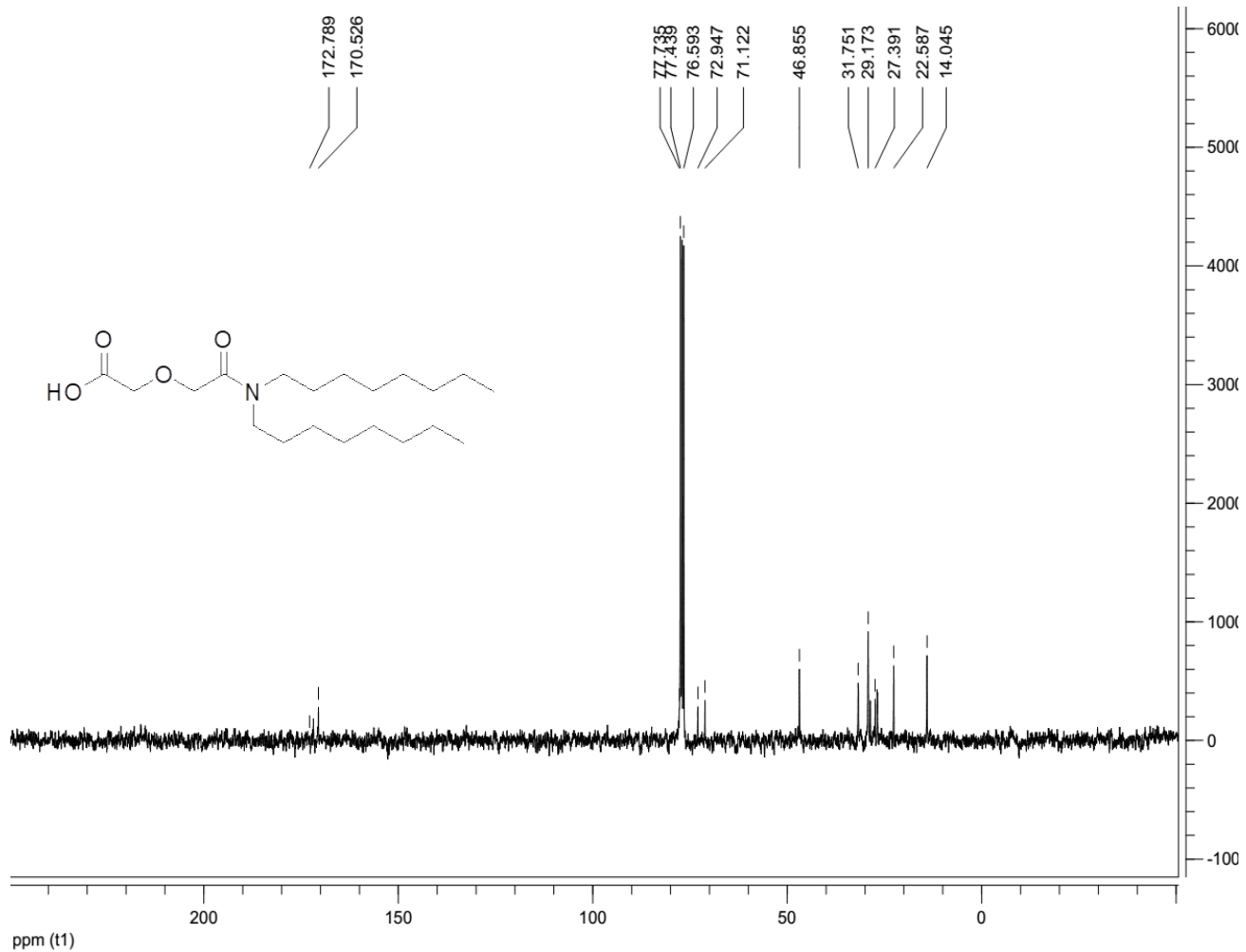


Fig. S3:  $^{13}\text{C}$ -NMR spectra for DGAMA-OCT in  $\text{CDCl}_3$

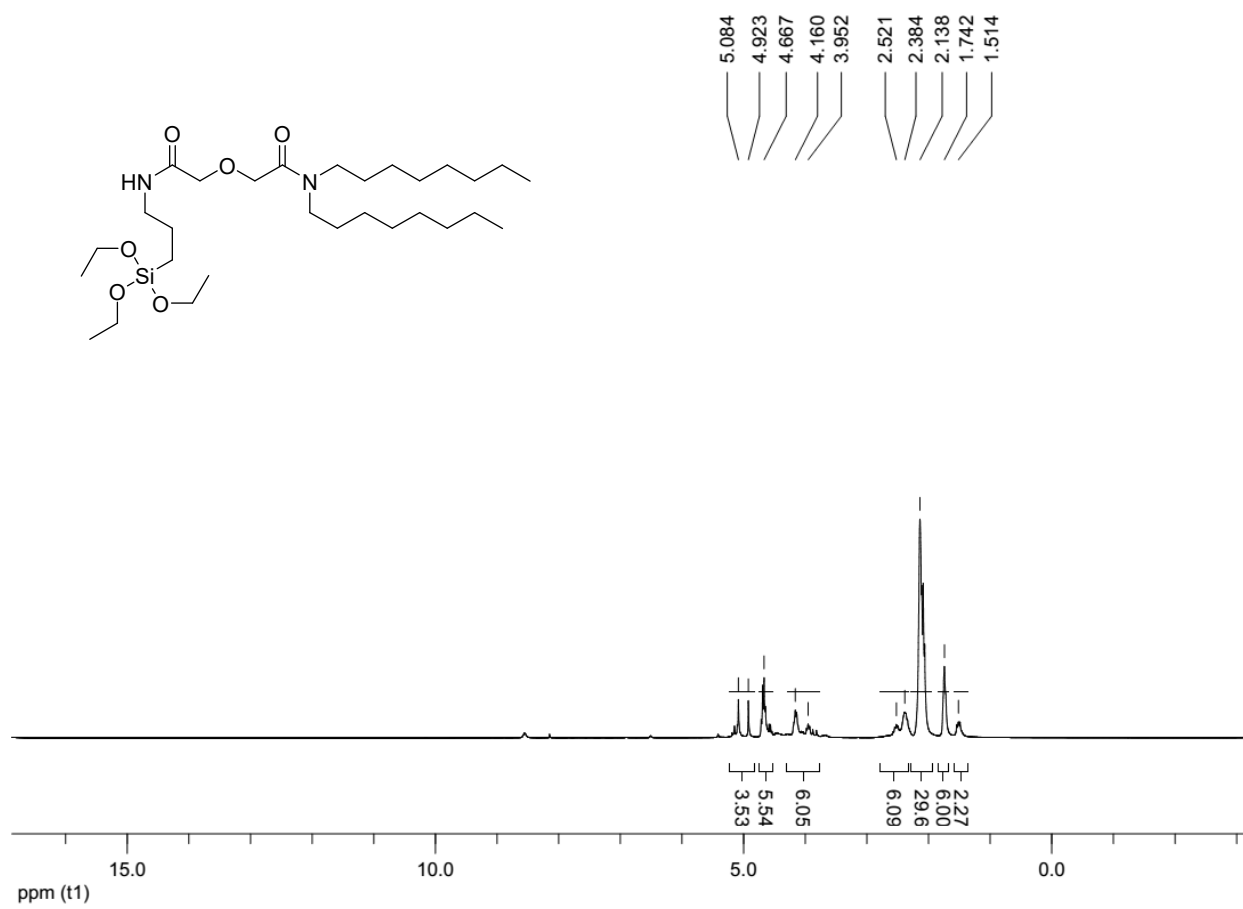


Fig. S4: <sup>1</sup>H-NMR of DGAMA-APTES-OCT in CDCl<sub>3</sub>

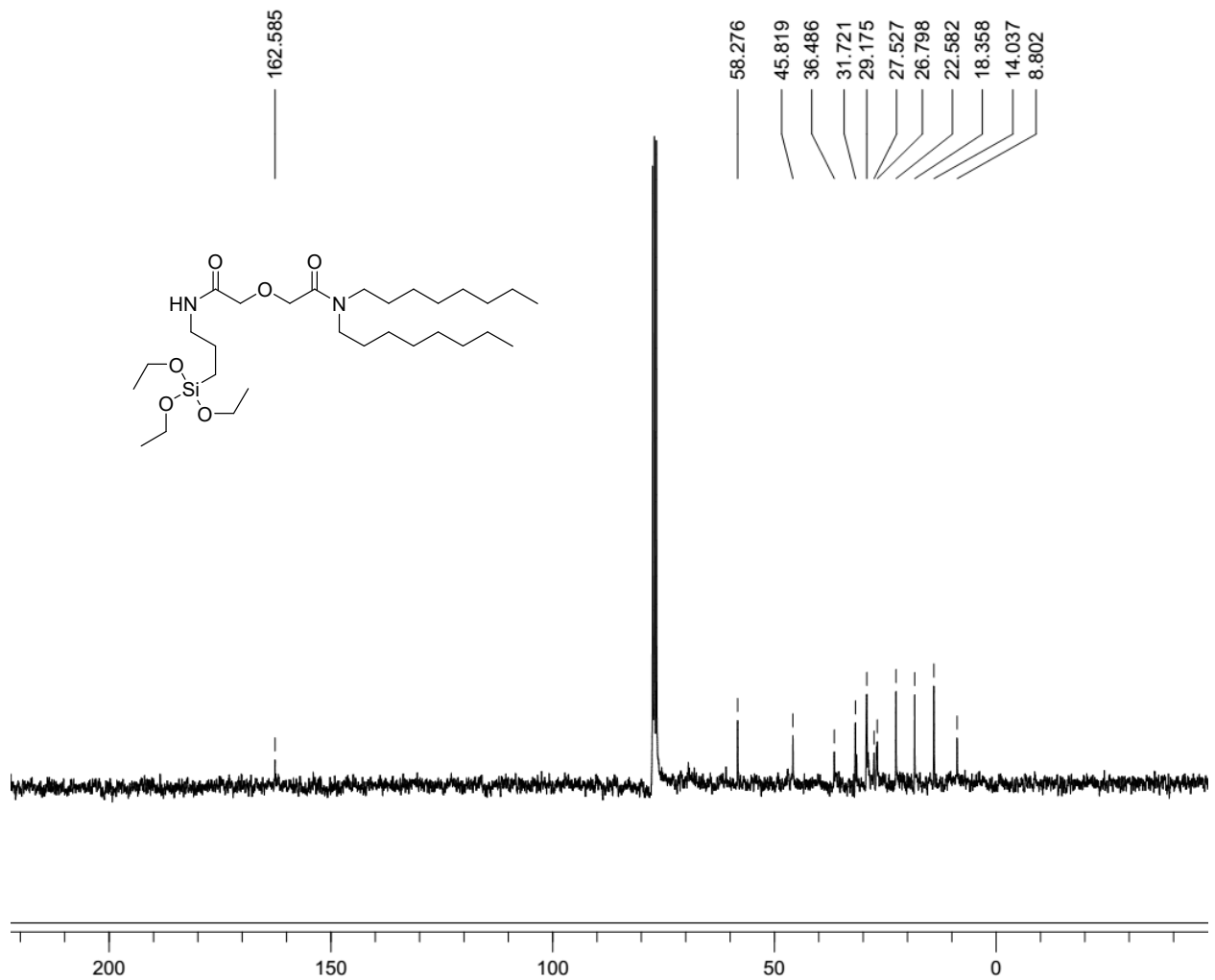


Fig. S5:  $^{13}\text{C}$ -NMR of DGAMA-APTES-OCT in  $\text{CDCl}_3$

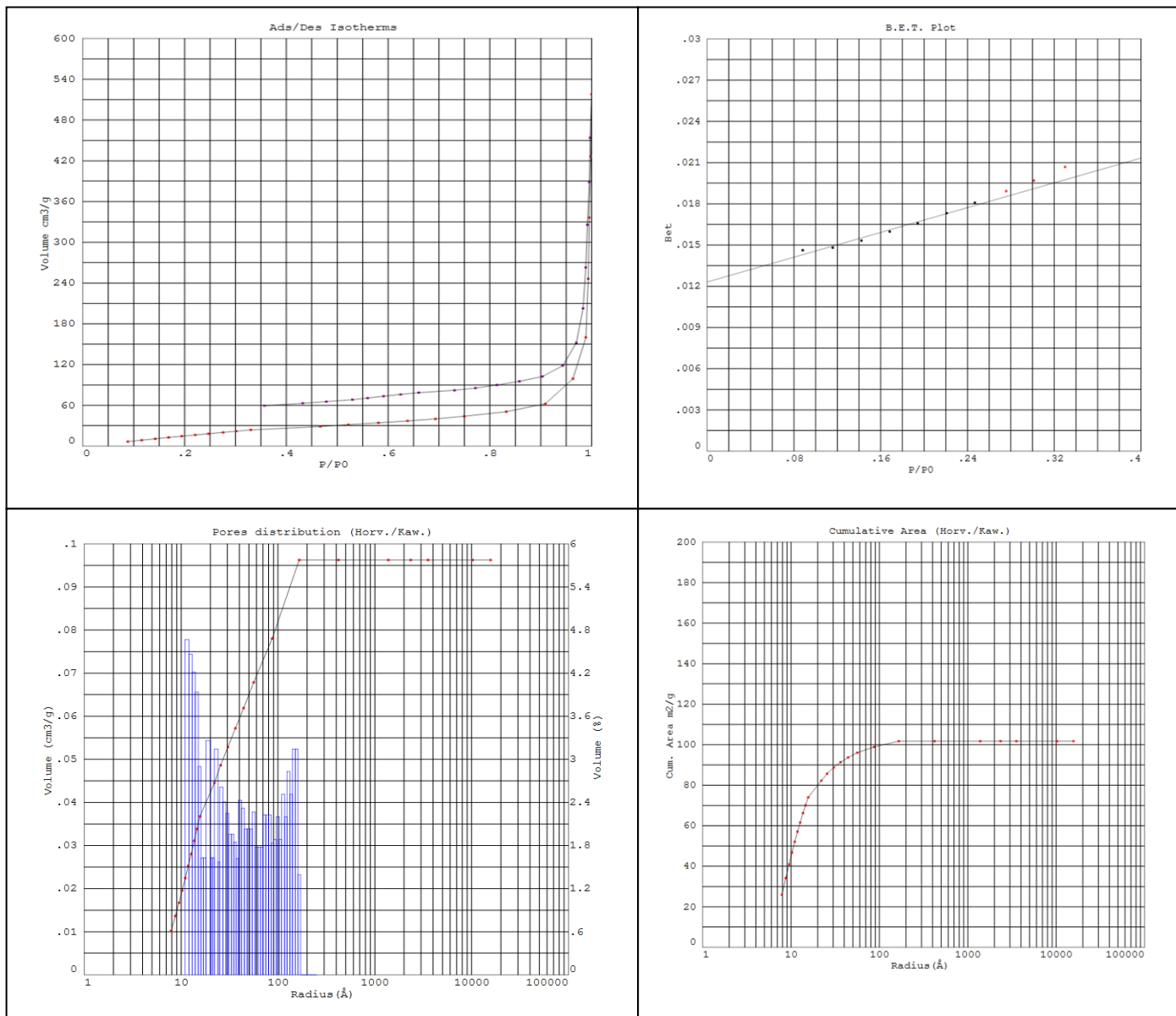


Fig. S6: N<sub>2</sub> adsorption- desorption study and BET analysis for Fe<sub>3</sub>O<sub>4</sub>MNP

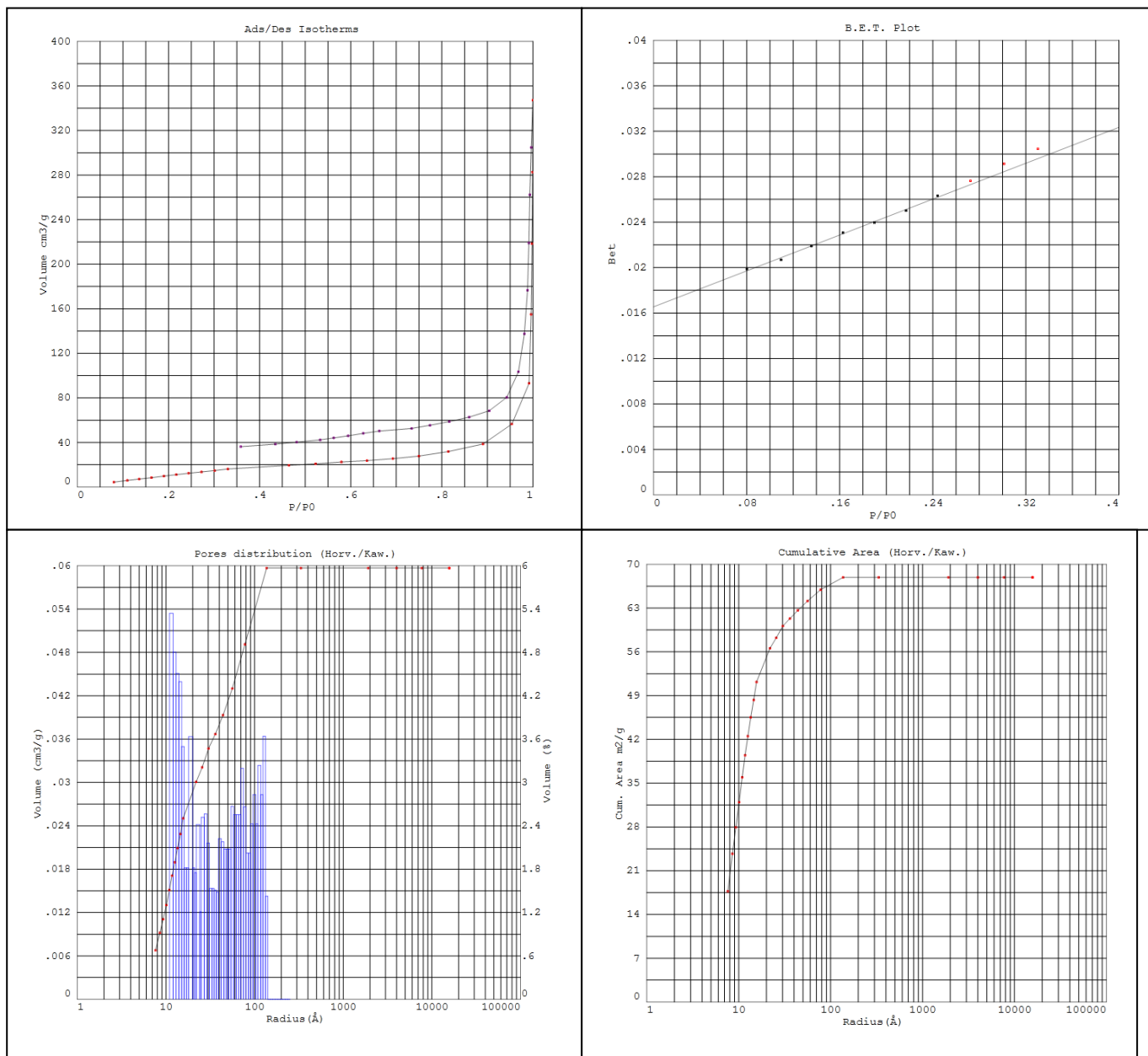


Fig. S7: N<sub>2</sub> adsorption- desorption study and BET analysis for silica coated core shell Fe<sub>3</sub>O<sub>4</sub> MNP

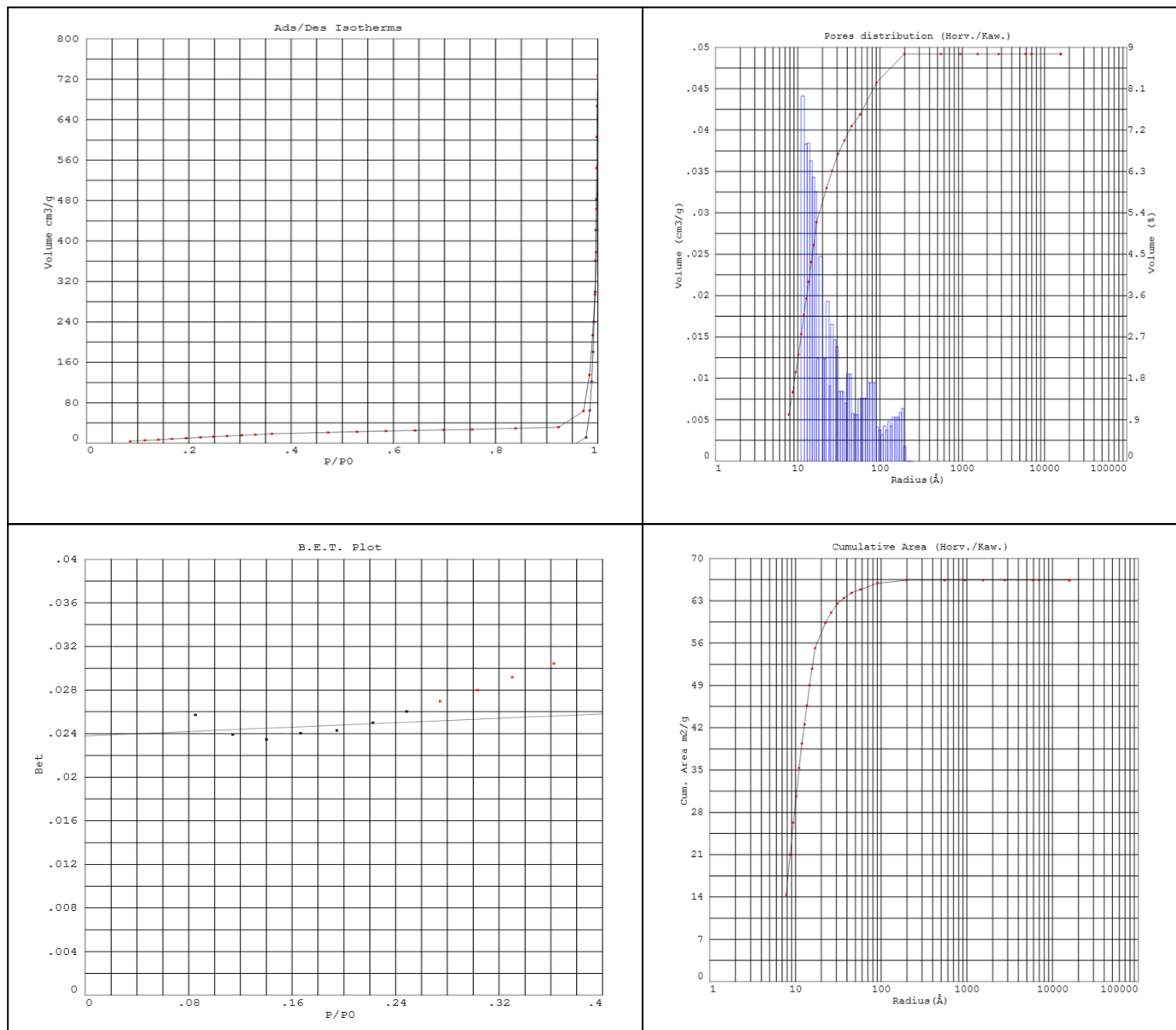


Fig. S8: N<sub>2</sub> adsorption- desorption study and BET analysis for MNSCDGA



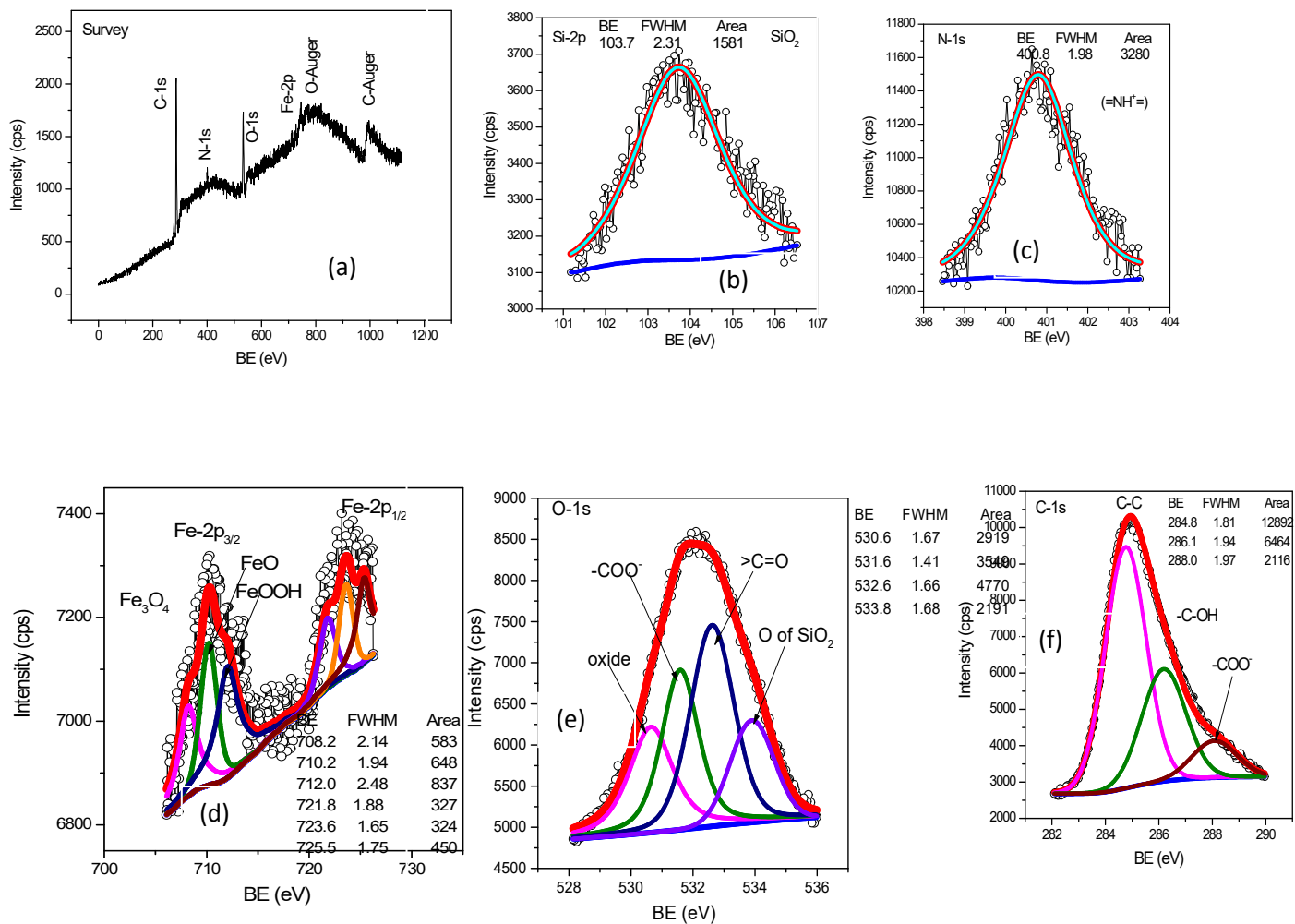


Fig. S9: XPS analysis for DGAMA-APTES-OCT (a) Full spectra in the range of 0-1100 eV; (b) Deconvoluted spectra for Si<sup>2P</sup>; (c) Deconvoluted spectra for N<sup>1s</sup>; (d) Deconvoluted spectra for Fe<sup>2P</sup>; (e) Deconvoluted spectra for O<sup>1s</sup>; (f) Deconvoluted spectra for C<sup>1s</sup>

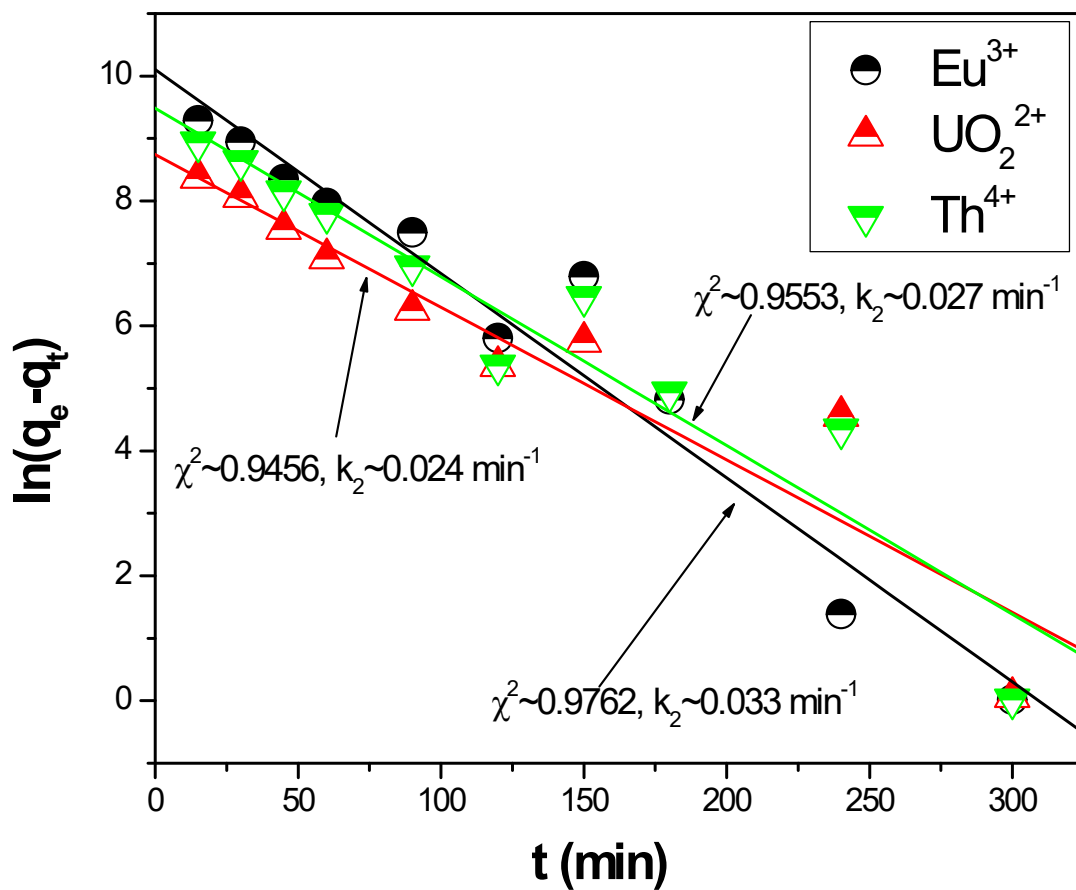


Fig. S10: Linear regression analysis for Lagergren 1<sup>st</sup> order rate kinetics for the sorption of Eu, U and Th

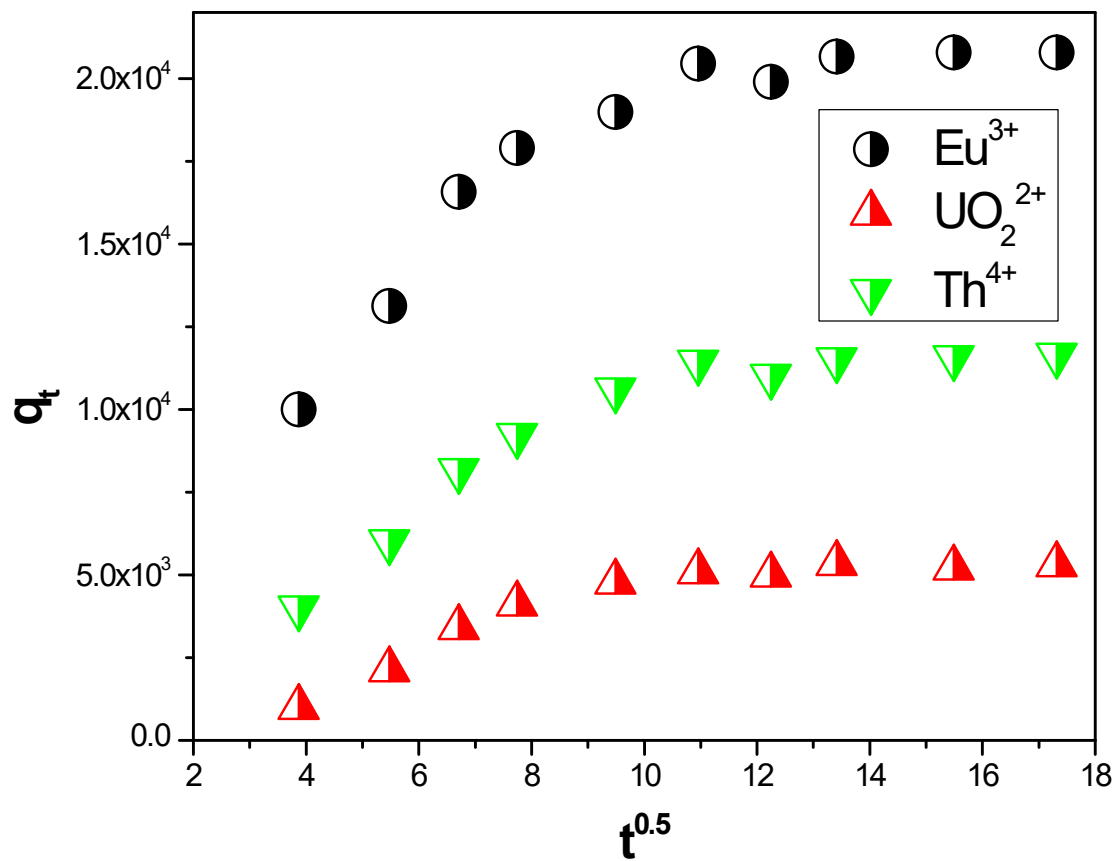


Fig. S11: Linear regression analysis for Intra particle diffusion kinetics for the sorption of Eu, U and Th

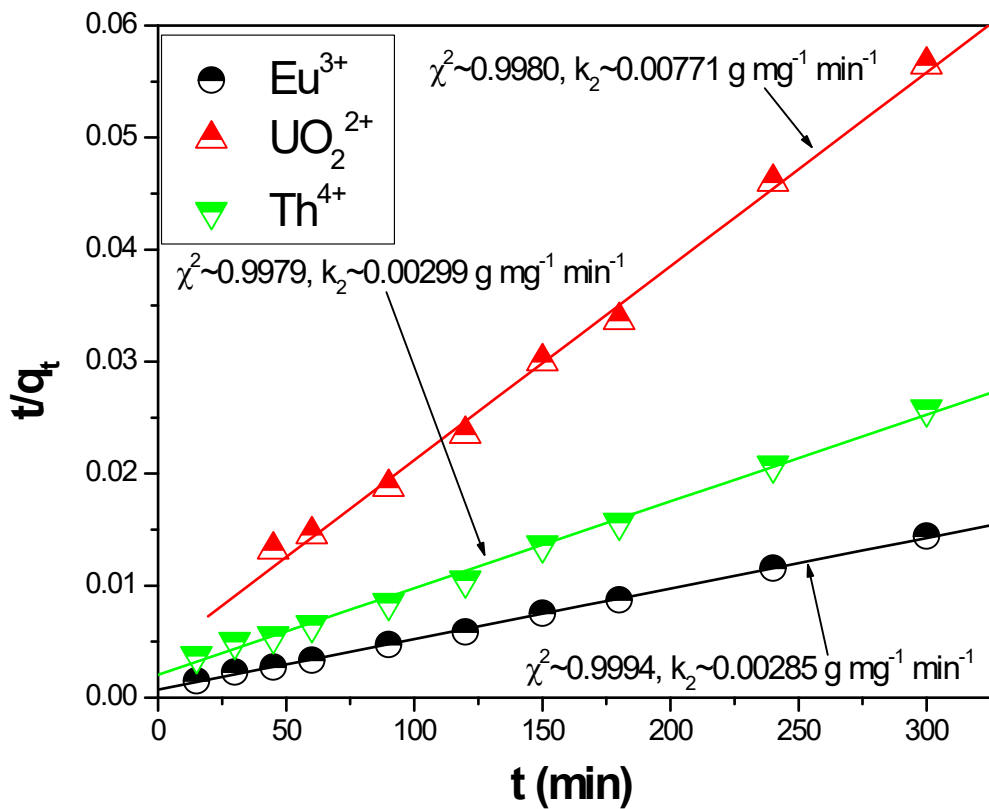


Fig. S12: Linear regression analysis for Pseudo2<sup>nd</sup> order rate kinetics for the sorption of Eu, U and Th

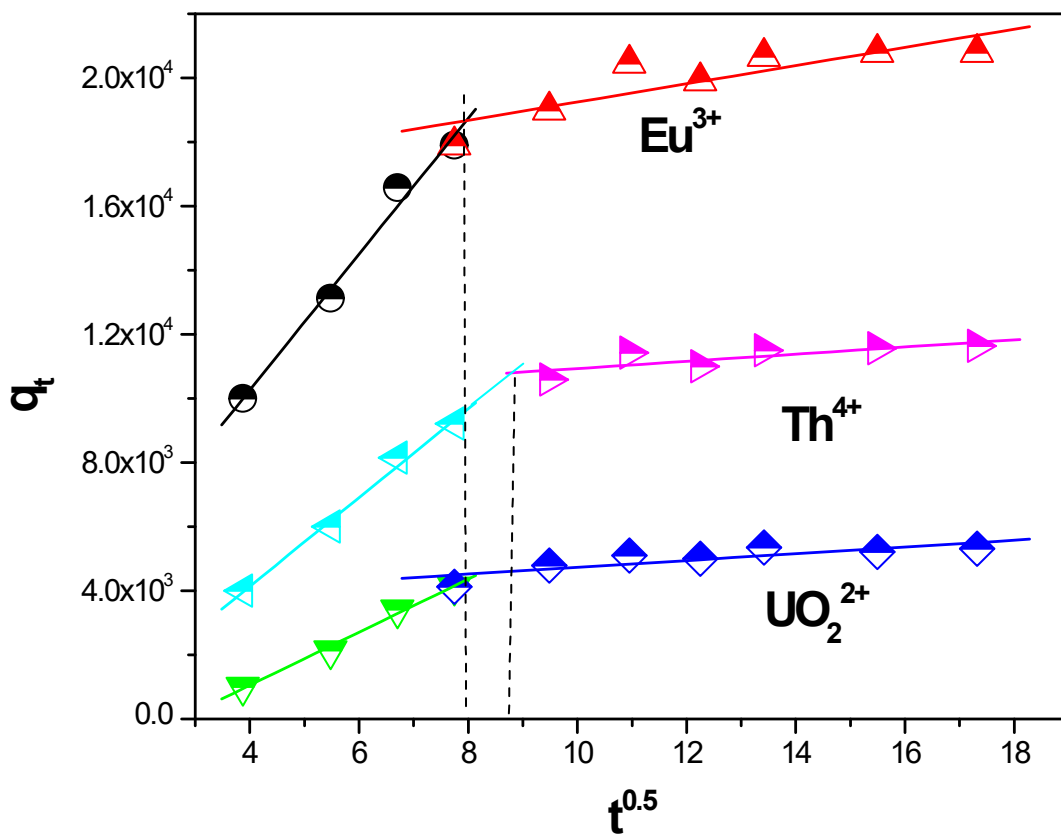


Fig. S13: Linear regression analysis for Weber-Morris model for the sorption of Eu, U and Th

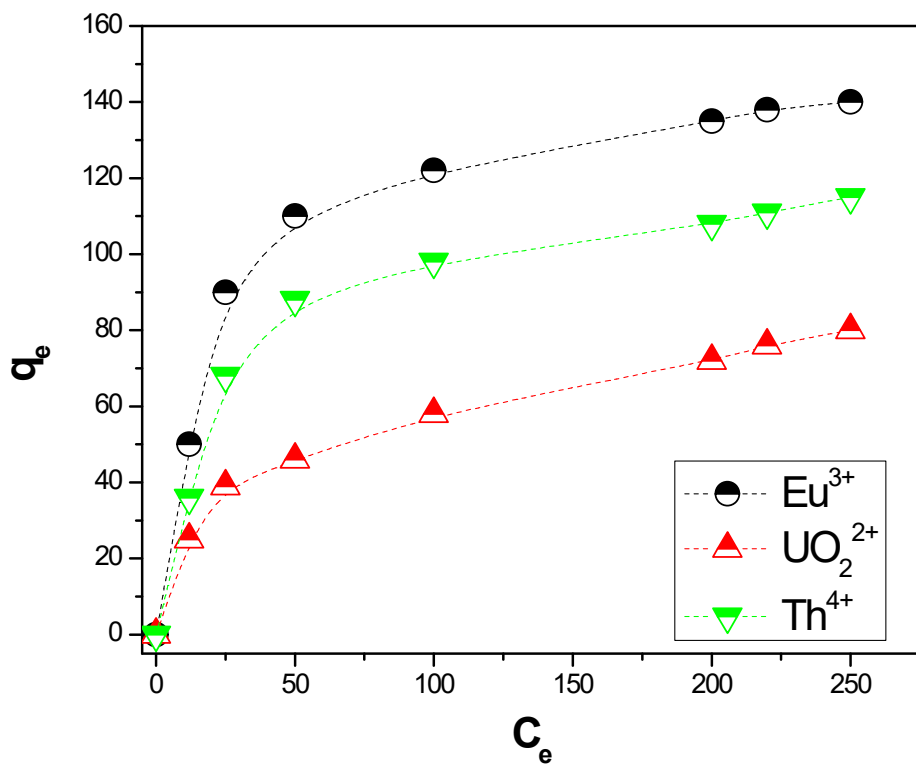


Fig. S14: Non-linear analysis of Langmuir isotherm for the sorption of Eu, U and Th

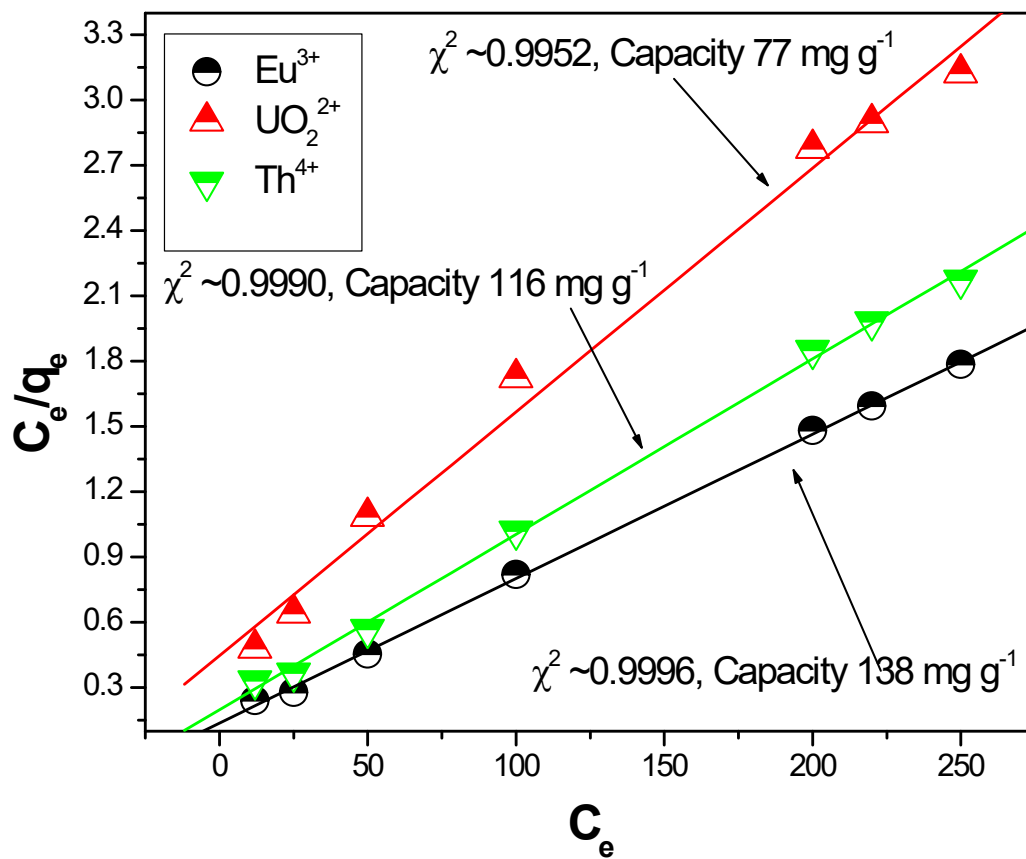


Fig. S15: Linear regression analysis of Langmuir isotherm for the sorption of Eu, U and Th

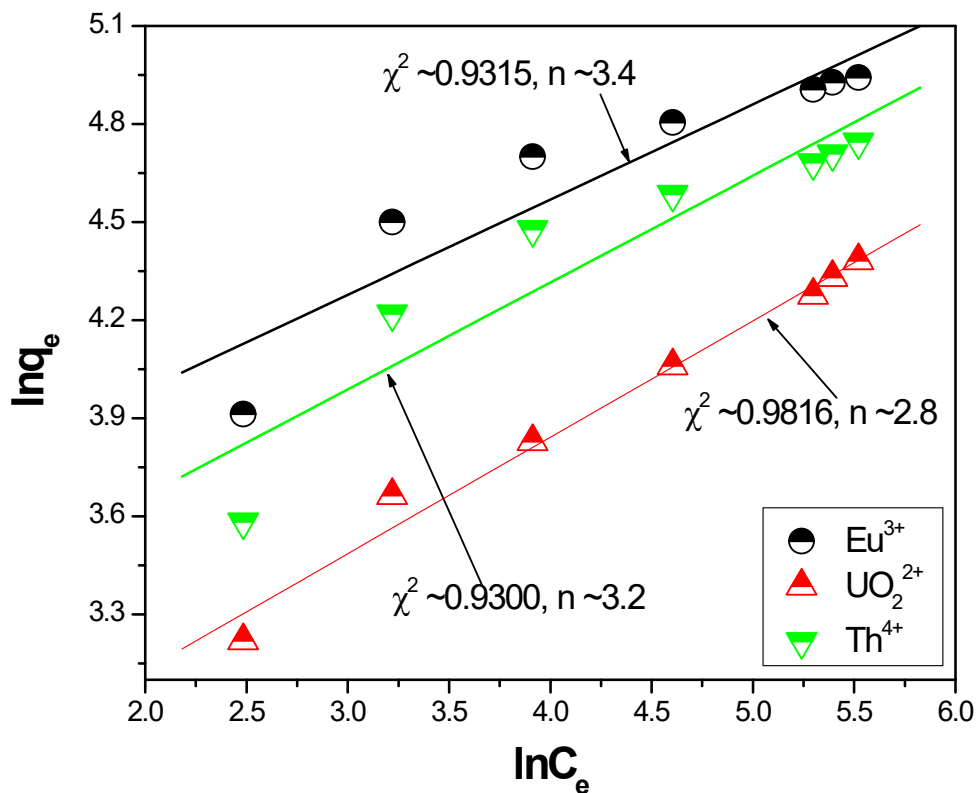


Fig. S16: Linear regression analysis of Freundlich isotherm for the sorption of Eu, U and Th

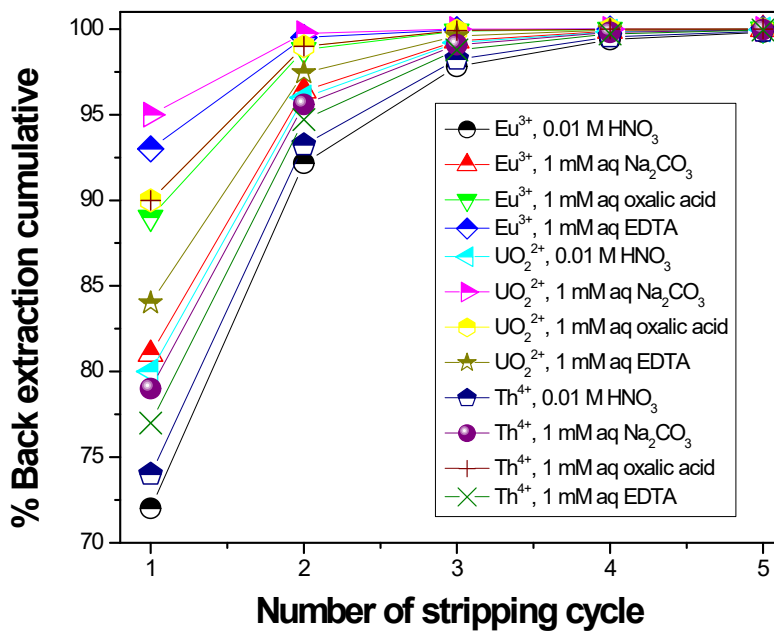


Fig. S17: Cumulative back extraction of f-block cations from loaded solid phase using different aqueous phase complexing agents



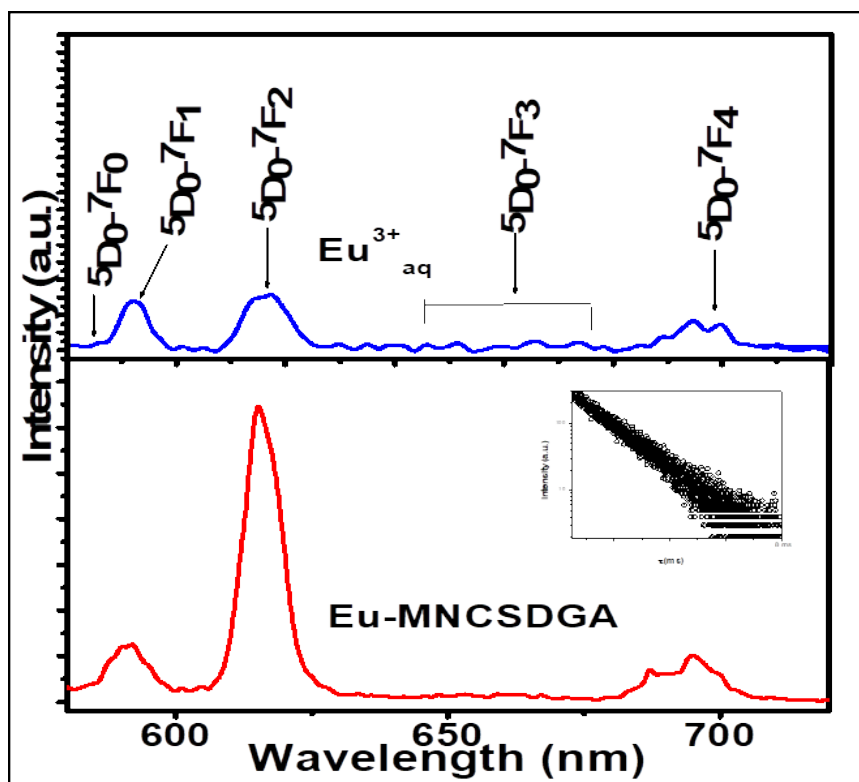


Fig. S18: Luminescence spectra of  $\text{Eu}^{3+}$  aq. & Eu MNCSDGA

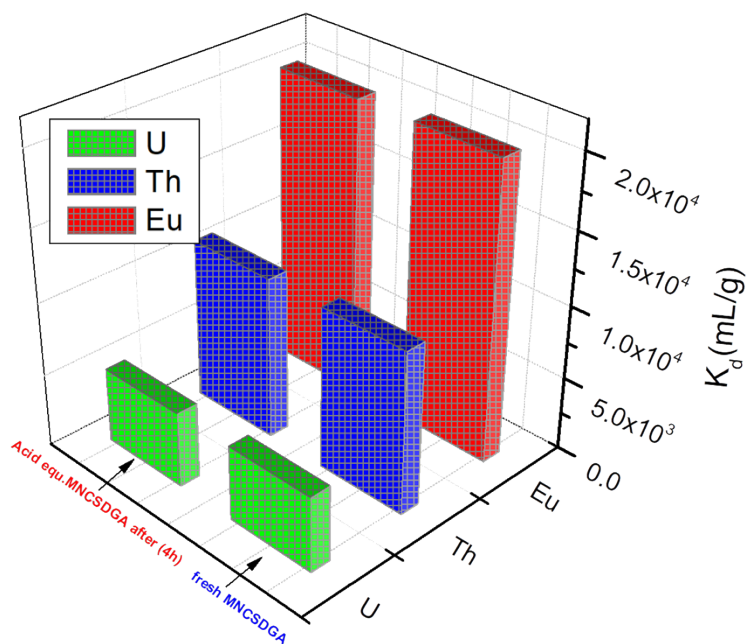


Fig. S19:  $K_d$  (mL/g) values of Eu, Th, & U from 4.0 M  $\text{HNO}_3$  before and after 4h of acid equilibration

Table S1: The separation factor of common metal ions over Eu, U and Th

Material	Specific surface area (m <sup>2</sup> g <sup>-1</sup> )	pore specific volume(cm <sup>3</sup> g <sup>-1</sup> )	maximum pore volume (cm <sup>3</sup> g <sup>-1</sup> )	C Value BET	Co-relation factor
Fe <sub>3</sub> O <sub>4</sub> MNP	124.93	0.096	0.096	2.83	0.9890
Silica coated Fe <sub>3</sub> O <sub>4</sub> MNP	77.69	0.060	0.060	3.38	0.9983
MNCSDGA	150.77	0.049	0.049	1.21	0.3081

Table S2: The separation factor of common metal ions over Eu, U and Th

Metal ion (X)	$\beta_{Eu/X}$	$\beta_{U/X}$	$\beta_{Th/X}$
Na <sup>+</sup>	355.3	89.3	196.4
K <sup>+</sup>	301.5	75.8	166.6
Ca <sup>2+</sup>	49.8	12.5	27.5
Mg <sup>2+</sup>	43.2	10.9	23.9
Fe <sup>3+</sup>	28.43	7.1	15.7
Cr <sup>3+</sup>	29.9	7.5	16.5
Mn <sup>2+</sup>	46.3	11.6	25.6

Table S3: Comparative picture of sorption behaviour different magnetic materials

Material	Sorption capacity (mg/g)			Operating medium	Stability in nitric acid	Ref
	U	Th	Eu			
GEMNPs	47.28	45.48	32.2	pH	No	22
Fe <sub>3</sub> O <sub>4</sub> @SiO <sub>2</sub> /P (TRIM-VPA)	60.4	*	*	4.0 M HNO <sub>3</sub>	Yes	23
Fe <sub>3</sub> O <sub>4</sub> @C@ASA	46.2	*	*	pH	No	24
Fe <sub>3</sub> O <sub>4</sub> @MCM-41-PDA/OA	38.11	*	25.4	pH	No	25
Fe <sub>3</sub> O <sub>4</sub> @MnO <sub>2</sub> hollow spheres	13.95	*	*	pH	No	26
Octadecylphosphonic acid bilayer@MnFe <sub>2</sub> O <sub>4</sub> NPs	1000	*	*	pH	No	27
Oleyl phosphate bilayer@MnFe <sub>2</sub> O <sub>4</sub> NPs	1667	*	*	pH	No	27
Phosphated-Fe <sub>3</sub> O <sub>4</sub> NPs	1690	*	*	pH	No	28
Fe <sub>3</sub> O <sub>4</sub> @ZIF-8	523.5	*	*	pH	No	10a
MNSCDGA	77	116	138	4.0 M HNO <sub>3</sub>	Yes	This work
*not reported						

## Equation(s)

- i. Lagergren 1<sup>st</sup> order:  $\ln(q_e - q_t) = \ln q_e - k_1 t$ , Here,  $q_e$  and  $q_t$  (mg/g) are the adsorptive removal capacity at equilibrium and variable time (t), respectively.  $k_1$  is the rate constant
- ii. Pseudo 2nd order:  $\frac{t}{q_t} = \frac{1}{k_2 q_e^2} + \frac{t}{q_e}$ ; Where,  $q_t$  and  $q_e$  are the amount of metal ion adsorbed at equilibrium and at time t,  $k_2$  is the pseudo 2nd order rate constants.
- iii. Intra-particle diffusion kinetics:  $q_t = k_f \sqrt{t} + C$ ;  $k_f$  is the intraparticle diffusion rate constant and C is the intercept
- iv. Langmuir isotherm:  $\frac{C_e}{q_e} = \frac{1}{Q_0 b} + \frac{C_e}{Q_0}$ ; where  $q_e$  (mg/g) and  $C_e$  (mg/L) are the amount of adsorbed metal ion per unit mass of adsorbent and unadsorbed metal ion concentration in solution at equilibrium, respectively.  $Q_0$  (mg/g) is the maximum amount of metal ion per unit mass of sorbent to form a complete monolayer on the surface bound at high  $C_e$  and  $b$  is a constant related to the affinity of the binding sites.
- v. Freundlich Isotherm:  $\log q_e = \log K_f + \frac{1}{n} \log c_e$ ; where  $K_f$  and  $n$  are Freundlich constants;  $K_f$  (mg/g (L/mg)<sup>1/n</sup>) being the sorption capacity of the adsorbent, and  $n$  giving an indication the favorability of the sorption process. Values of  $n > 1$  represent favorable adsorption condition
- vi.  $N_{H_2O} = \frac{1.05}{\tau} - 0.7$ ; where  $N_{H_2O}$ , stands for number of water molecule and lifetime of the luminescence decay
- vii. Asymmetry factor =  $\frac{I_{5D_0 \rightarrow 7F_1}}{I_{5D_0 \rightarrow 7F_2}}$ ; I stands for intensity of respective emission lines.

## Reference:

1. P.P. Barthelemy, G.R. Choppin, Luminescence study of complexation of europium and dicarboxylic acids, *Inorg. Chem.*, 28 (1989) 3354–3357.
2. H. Zheng, D. Liu, Y. Zheng, S. Liang, Z. Liu, Sorption isotherm and kinetic modeling of aniline on Cr-b entonite, *J. Hazard. Mater.*, 167 (20 09) 141–147.